Hittite Journal of Science and Engineering, 2020, 7 (4) 287–296
ISSN NUMBER: 2148–4171
DOI: 10.17350/HJSE19030000198

Mineral Chemistry–thermobarometry and Petrography of Metamorphic Sole Rocks of Kömürhan Ophiolite (SE Turkey): Constraints to Evolution and Emplacement

Nusret Nurlu
Cukurova University, Department of Geological Engineering, Adana, Turkey

ABSTRACT

This paper presents the generation of metamorphic sole rocks through the detailed geochemical and petrographical analysis of field work carried out on the Kömürhan ophiolite. The metamorphic sole rocks of Kömürhan ophiolite are defined as amphibolite (Pl+Mg–Hbl+Ttn±Ap) plagioclase–amphibole schist (Pl+Mg–Hbl+Cpx+Ttn±Zrn±Ap), plagioclase–clinopyroxene–amphibole schist (Pl+Di+Mg–Hbl+Ttn±Ap), and epidote–plagioclase amphibole schist (Ep+Pl+Mg–Hbl+Ttn±Ap±Qtz±Zrn). This research mainly reports comprehensive petrography and mineral chemistry analyses of metamorphic sole rocks of Kömürhan ophiolite of SAOB (Southeast Anatolian Orogenic Belt) together with a goal of presenting geothermobarometric examination and unravelling the mineral systematics. The metamorphic sole rocks have been observed as a thin slice and these rocks are seen at the base of the tectonites, metamorphosed in amphibolites facies throughout the intra–oceanic supra-subduction geodynamic environment. The Kömürhan ophiolite includes from the top to bottom volcanics, sheeted dike complex, isotropic gabbros cumulates, and tectonites and shows a complete oceanic lithospheric fragments. Analyses of mineral chemistry and petrography of metamorphic sole rocks have been used to exhibit the metamorphic processes of these rocks. Mineral chemistry analyses of pyroxene phenocrysts in the metamorphic sole rocks of Kömürhan ophiolite present similarities island arc tholeiite (IAT), proposing that protolith of the sole rocks was related to the supra-subduction geodynamic environment. The amphibolites were occurred by metamorphism of island arc tholeiite–type volcanics that separated from the front of the obducted ophiolite (Kömürhan ophiolite) and after that underplated.

Article History:
Received: 2020/06/05
Accepted: 2020/11/08
Online: 2020/12/31

***Correspondence to**: Nusret Nurlu,*
Cukurova University, Geological Engineering, 01330, Balcali, Adana, Turkey
E-Mail: nusretnurlu@gmail.com
Phone: +90 322 338 70 81
Fax: +90 322 338 70 81

Keywords:
Mineral chemistry; Kömürhan ophiolite; Amphibolites; Petrography; Metamorphic sole; Thermobarometry

INTRODUCTION

Slim sheets of the metamorphic sole rocks related to ophiolitic bodies were presented by many researchers and numerous ophiolitic bodies hold amphibolite at their sole which includes a clear inverted grade of metamorphism. [e.g. 1, 2, 3, 4]. These mainly amphibolite rocks are believed to have occurred throughout the emplacement and detachment of the ophiolite. The Kömürhan ophiolite holds the amphibolites of metamorphic sole rocks in the SAOB. Many publications have reported the presence of metamorphic sole rocks beneath several ophiolitic complexes of the Tethys, including Baer–Bassit in Syria [5, 11, 12], Mersin in south Turkey [6, 7, 8], and Pozanti–Karsantı in Turkey [13]. One of the best–preserved examples is Semail in Oman [3, 14, 9, 10]. The ophiolitic bodies of the eastern Mediterranean district in southern Turkey comprise two main features: (i) the SAOB and (ii) the Inner Tauride Suture Zone. The SAOB also includes the Bitlis–Zagros thrust belt and folds that include pristine oceanic lithosphere from the southern branch of Neo–Tethys, especially Troodos, Kızıldağ, İspendere, Guleman and Bear-Bassit in Syria. The Neo–Tethyan duration of the SAOB started in the Triassic (by rifting) and finished in the Miocene, with the collision of the Tauride plate and the Arabian plate [15, 16, 17, 18, 19, 48]. The Southeast Anatolian Orogenic belt includes important examples of unmetamorphosed ophiolites (given from west to east): Göksun, Meydan (Kahramanmaraş), İspendere, Kömürhan (Malatya), and Guleman (Elazığ), observed in the north, and also the Koçali (Adıyaman) and Kızıldağ (Hatay) ophiolites, observed in the south (Fig. 1) [16, 17, 20, 21, 22, 18, 19, 23, 24, 25, 26, 4]. The study area is placed in the area among Sivrice

and Baskil (Elazığ) regions. The outcrops of the rocks forming the Kömürhan ophiolite and related metamorphic sole rocks which are the main subject of this paper start from the Kömürhan Bridge and continue to the west of Sivrice town (Elazığ), mainly along the Malatya-Elazığ highway (Fig. 1b).

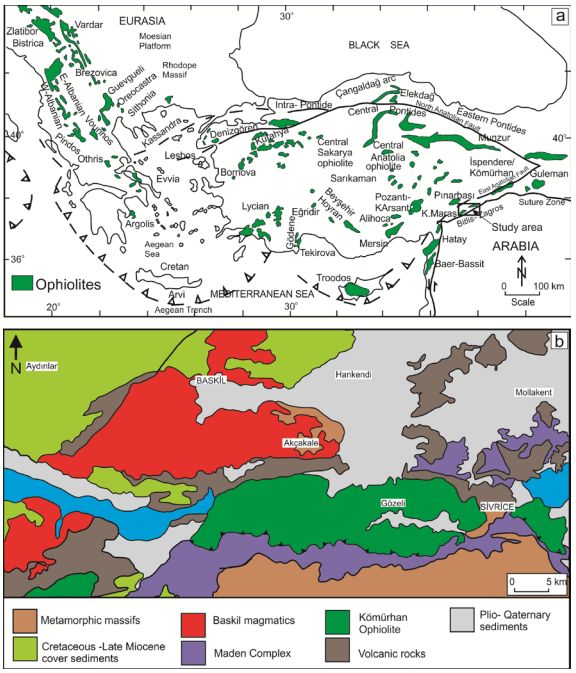

Figure 1. a) Neo–Tethyan ophiolites in the eastern Mediterranean region (from [27, 23]. b) Simplified geological map of the Kömürhan ophiolite (Malatya–Elazığ region), simplified from [28].

The whole–rock geochemistry, geochronology, and petrology of Kömürhan ophiolite and are properly described [23, 29]. However, a detailed examination of mineral chemistry, petrography and field relations of metamorphic sole rocks of Kömürhan ophiolite is yet reported. The principal objectives of this paper are to: (a) yield mineral chemistry of the metamorphic sole rocks; (b) report the geodynamic setting, protolith and geothermobarometric development of metamorphic sole rocks and also mineral data; and (c) summarise the geodynamic environment of the Kömürhan ophiolite during the development of the Southeast Anatolian Suture Zone of the Neo–Tethyan oceanic region within the eastern Mediterranean tectonic roof.

GEOLOGICAL SETTING

The ophiolitic unit is observed in an area of approximately 135-140 km² [23, 29]. The Kömürhan ophiolite is located on the Middle Eocene-aged Maden Complex south of the Kömürhan Bridge, with an overlapping contact relationship outside of the study area. It is unconformably overlain by the late Paleocene–early Eocene Seske formation. The Kömürhan ophiolite is also cut by the Upper Cretaceous aged Baskil granitoid, which provides wide dispersions in the region [23, 29]. This intrusive contact relationship has been developed synthinematically in places (Fig. 2–3). The mineral chemistry data of clinopyroxenes are various and yields a filtered appearance of the contents of the protolith from which the clinopyroxene crystallized, lending it the prospective to give insight into the geodynamic environment of metamorphic sole rocks of Kömürhan ophiolite. Metamorphic sole rocks are observed in the Kömürhan Bridge and Karakaya Hill in a fairly narrow area, approximately 250–280 meters thick. The examined metamorphic sole rocks consist of a reverse zoned metamorphic slice that varies from green–schist facies to amphibolite facies. Although the unit is observed directly on the basis of ultramafic cumulates, due to the effectiveness of tectonism, the normal stratigraphic sequence is distorted as a result of occasional tilting [23, 29]. The examined rocks belonging to the metamorphic sole rocks are mainly represented by amphibolite, plagioclase–amphibolite schist, plagioclase–clinopyroxene-amphibole schist, and epidote–plagioclase amphibole schist and especially schist type metamorphic rocks are remarkable because they have a macroscopically distinct schistosity and present alterations colours in shades of green (Fig. 3).

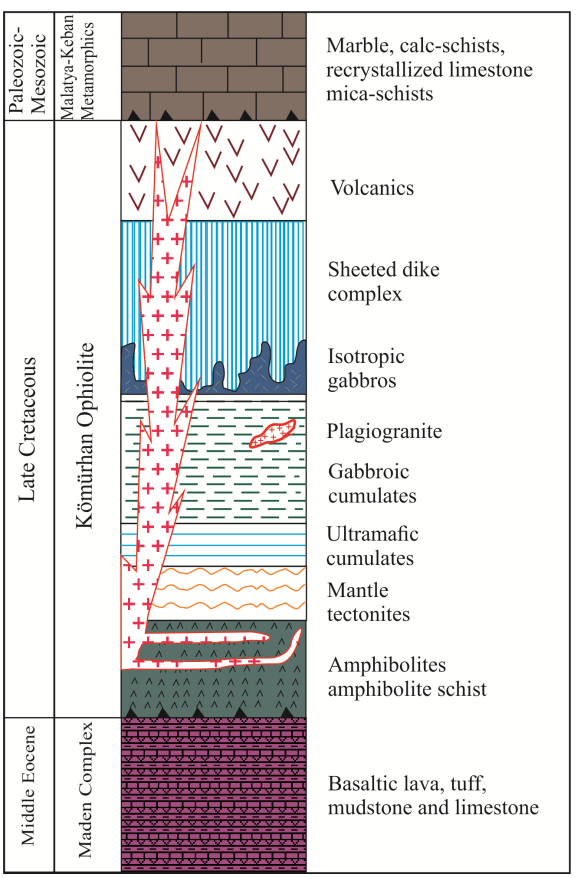

Figure 2. Synthetic log of the Kömürhan ophiolite (from [23, 29])

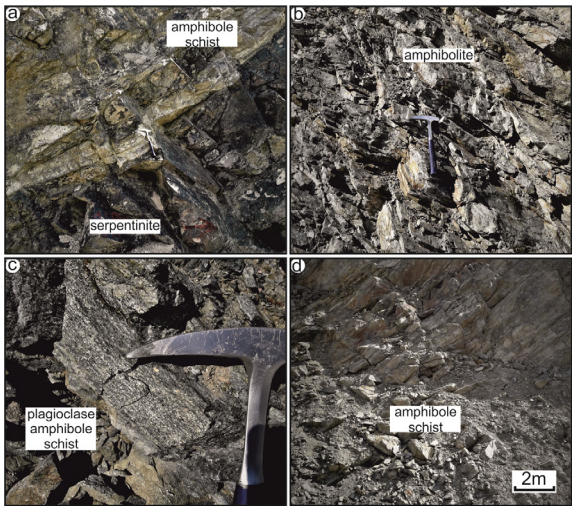

Figure 3. Field photographs of the metamorphic sole rocks and serpentinites of Kömürhan ophiolite. (a) A tectonic relation with the amphibolites and serpantinites the in the Kömürhan ophiolite. (b) General view of amphibolites of metamorphic sole rocks of Kömürhan ophiolite. (c) Plagioclase amphibole schist (d) Field observation of the amphibole schist.

MATERIAL AND METHODS

Petrographical analyses

The metamorphic sole and mafic dike rock types were initially examined in thin section handling an optical microscope (ca. 115 thin sections) and conducted the sampling of rocks suitable for petrological analysis.

Electron microprobe analyses

Thin sections (about 30 microns thick) for four samples were prepared by the EAS Thin Section Laboratory at the Department of Earth and Atmospheric Sciences (EAS) at the University of Alberta. Major element compositions of minerals and phase relationships were studied by electron microprobe at the EAS at the University of Alberta (Canada). The operating conditions were; 40 degrees take off angle, accelerating voltage 20 kV, beam current 20 nA, and beam diameter <1 micron (fully focused), except on the zeolite points that were run separately with a 10-micron diameter beam. The Kα X-ray lines of 13 elements were measured using the following diffraction crystals: PET (pentaerythritol) – P, K, Ca, Ti, V, Cr; TAP (thallium hydrogen phthalate) – Na, Mg, Al, Si; LIF (lithium fluoride) – Mn, Fe, Ni. Total count times of 30 seconds were used for both emission peaks and background positions for all elements except Na, for which 60 seconds was used. Interference corrections were applied to V for interference by Ti, and to Cr for interference by V, and to Mn for interference by Cr [24]. Intensity data were reduced according to [25] and the choice of mineral standards varied with the mineral analysed. Oxygen was calculated by stoichiometry and included in the data reduction.

Representative data are shown in Tables 1–4. Detailed mineral chemistry analyses of 35 points on clinopyroxene, plagioclase, titanite and amphibole minerals were carried out on 2 samples from the rocks belonging to the metamorphic sole observed in the Kömürhan ophiolite (Table1–4).

PETROGRAPHY AND MINERALOGY

Amphibolites have a darker green alteration surface, are generally massive and are observed to be more strength compared to schist type rocks. Detailed petrographic properties reported as a result of thin section determination studies on metamorphic sole rocks compiled in the study area are given below. The amphibolites in the study region are represented by plagioclase, hornblende, epidote, titanite and ± zircon ± opaque minerals such as magnetite. These rocks present generally nematoblastic and granoblastic textures and are commonly dark green coloured. Calcite, prehnite, and quartz are mainly seen in the vein of the amphibolite type rocks. Feldspars are commonly represented by plagioclases and these minerals present various degrees of alteration. Though, non-altered plagioclases showing polysynthetic twinning have been seen.

Pyroxenes are represented by diopsides and they have been seen as relicts in most of the amphibolites. The plagioclase-amphibolite schists present nematoblastic texture and consist of green hornblende (50-55 vol%), plagioclase (30–35 vol%) and rare quartz, opaque minerals (Fig. 4a). The epidote-plagioclase amphibole schist present epidote (7–8 vol%), plagioclase (30–35 vol%) and hornblende (50–55 vol%) and has nematoblastic texture. Serpentinized wherlites are described as rocks holding olivine (45-55 vol%), serpentinite (20–25 vol%), and clinopyroxene (20–25 vol%). A

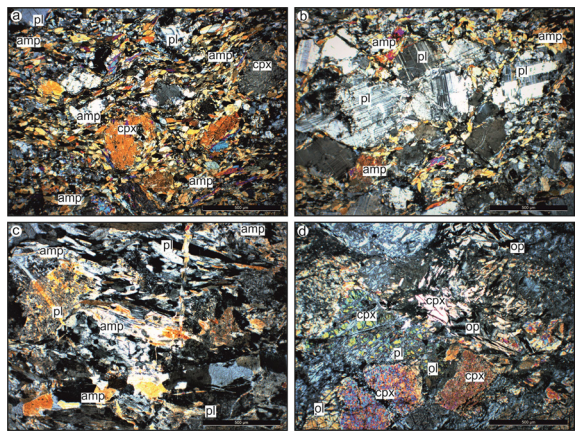

Figure 4. (a) Nematoblastic, granoblastic textures in the amphibolite. (b) Plagioclase porphyroblast in the schists. (c) Nematoblastic texture in the plagioclase-amphibole schist. (d) serpentinized wherlite presenting granular and mesh textures (abbreviations: cpx, clinopyroxene; pl, plagioclase; amp, amphibole; ol, olivine).

Table 1. Composition of the amphibole from the metamorphic sole rocks of Kömürhan ophiolite.

Sample	KMP-1	KMP-2	KMP-3	KMP-4	KMP-5	KMP-6	KMP-7	KMP-8	KMP-9	KMP-10	KMP-11
SiO_2	53.05	54.63	54.84	53.74	54.74	54.57	54.62	54.86	54.54	53.73	54.02
TiO_2	0.48	0.04	0.04	0.34	0.06	0.05	0.06	0.00	0.06	0.06	0.05
Al_2O_3	2.55	0.44	0.73	1.75	0.86	0.83	0.84	0.69	0.73	0.80	0.54
Cr_2O_3	0.19	0.00	0.06	0.20	0.07	0.00	0.03	0.00	0.04	0.10	0.04
FeO	4.84	4.85	4.46	4.36	4.44	5.02	4.99	4.43	4.63	4.84	4.91
MnO	0.17	0.19	0.17	0.19	0.18	0.21	0.20	0.18	0.21	0.18	0.19
MgO	14.78	15.34	15.35	15.15	15.48	14.97	14.95	15.41	15.07	15.12	15.20
CaO	23.37	24.72	24.63	24.26	24.66	24.54	24.49	24.83	24.66	24.57	24.69
Na_2O	0.37	0.15	0.24	0.27	0.21	0.20	0.24	0.23	0.20	0.24	0.17
K_2O	0.00	0.00	0.00	0.00	0.00	0.00	0.00	0.00	0.00	0.00	0.00
A	7.02	5.14	4.95	5.84	5.09	5.65	5.59	4.89	5.16	5.40	5.28
C	23.37	24.72	24.63	24.26	24.66	24.54	24.49	24.83	24.66	24.57	24.69
F	19.79	20.38	19.98	19.70	20.10	20.20	20.14	20.02	19.91	20.14	20.30
TOTAL	99.82	100.41	100.54	100.31	100.73	100.40	100.43	100.68	100.16	99.66	99.82
Si	1.95	2.00	2.01	1.97	2.00	2.00	2.00	2.00	2.01	1.98	1.99
Ti	0.01	0.00	0.00	0.01	0.00	0.00	0.00	0.00	0.00	0.00	0.00
Al	0.11	0.02	0.03	0.08	0.04	0.04	0.04	0.03	0.03	0.03	0.02
Fe^{+3}	0.00	0.00	0.00	0.00	0.00	0.00	0.00	0.00	0.00	0.01	0.00
Cr^{+3}	0.01	0.00	0.00	0.01	0.00	0.00	0.00	0.00	0.00	0.00	0.00
Fe^{+2}	0.15	0.15	0.14	0.13	0.14	0.15	0.15	0.14	0.14	0.14	0.15
Mn	0.01	0.01	0.01	0.01	0.01	0.01	0.01	0.01	0.01	0.01	0.01
Mg	0.81	0.84	0.84	0.83	0.84	0.82	0.82	0.84	0.83	0.83	0.84
Ca	0.92	0.97	0.96	0.95	0.96	0.97	0.96	0.97	0.97	0.97	0.98
Na	0.03	0.01	0.02	0.02	0.01	0.01	0.02	0.02	0.01	0.02	0.01
K	0.00	0.00	0.00	0.00	0.00	0.00	0.00	0.00	0.00	0.00	0.00
H	0.00	0.00	0.00	0.00	0.00	0.00	0.00	0.00	0.00	0.00	0.00
TOTAL	4.00	4.00	4.00	4.00	4.00	4.00	4.00	4.00	4.00	4.00	4.00
Wo	48.98	49.59	49.79	49.77	49.65	49.79	49.79	49.93	50.08	49.96	49.71
En	43.10	42.82	43.17	43.25	43.37	42.26	42.29	43.12	42.58	42.78	42.58
Fs	7.92	7.59	7.04	6.98	6.98	7.95	7.92	6.95	7.34	7.26	7.72
Total	100.00	100.00	100.00	100.00	100.00	100.00	100.00	100.00	100.00	100.00	100.00

Number of ions on the basis of six (O). *Total Fe is expressed as FeO.

few orthopyroxenes are rarely seen (Fig. 4d) and these rocks are presenting granular and mesh textures. The plagioclase-clinopyroxene-amphibole schist displays prominent foliation because of the preferred orientation of plagioclase (10–15 vol %), pyroxene (25–30 vol %), amphibole (40–45 vol %). The plagioclases are immensely altered to sericite and saussurite and these rocks also have accessory minerals such as apatite and zircon.

MINERAL CHEMISTRY

The EMPA (electron microprobe analyses) data for significative pyroxenes, amphiboles, biotites, and titanites from metamorphic sole rocks of Kömürhan ophiolites are given in Table 1-4. Formulae have been calculated on the basis of six (O) and twelve cations (including Na, K, Ca and H). In point of quadrilateral components, the clinopyroxene contents are $Wo_{48.9-49.7}$ $Fs_{6.95-7.95}$ $En_{42.3-43.4}$ in plagioclase-clinopyroxene amphibole schist. The Mg# of the clinopyroxenes are ranging from 0.846 to 0.861 (Table 2). Based on the Fe-Ca-Mg discrimination diagram of Morimoto (1989), the examined pyroxenes are fall in a distinct tight group on the Ca-rich limit of the diopside subfield (Fig. 5a). [32] suggested a set of basic discrimination diagrams in order to recognize the possible geodynamic environment of paleo-basalt on the basis of the mineral chemistry of clinopyroxenes. A series of diag-

Table 2. Composition of the pyroxene from the metamorphic sole rocks of Kömürhan ophiolite.

Sample	KMP-1	KMP-2	KMP-3	KMP-4	KMP-5	KMP-6	KMP-7	KMP-8	KMP-9
SiO2	50.95	49.4	50.76	51.19	49.32	50.01	52.65	50.45	49.51
TiO2	0.39	0.34	0.32	0.32	0.52	0.35	0.23	0.37	0.47
ZnO	0	0	0	0	0	0	0	0	0
Al2O3	6.82	8.4	7.22	6.93	8.46	7.72	5.53	7.82	7.66
Cr2O3	0.04	0.41	0.28	0.19	0.25	0.23	0.23	0.03	0.06
FeO	8.23	8.09	7.77	7.69	8.22	8.13	7.04	8.08	8.16
NiO	0.03	0.04	0.03	0	0.02	0.04	0.02	0	0.03
MnO	0.15	0.18	0.16	0.17	0.16	0.17	0.14	0.15	0.15
MgO	16.6	16.08	16.56	16.99	16.19	16.24	17.62	16.49	16.42
CaO	12.62	12.65	12.68	12.73	12.63	12.7	12.9	13	12.61
Na2O	1.03	1.17	1	1	1.32	1.08	0.7	1.08	1.19
K2O	0.01	0.02	0.01	0.01	0.02	0.01	0.01	0.02	0.01
TOTAL	96.87	96.77	96.82	97.24	97.11	96.67	97.09	97.53	96.28
Species	Mg-Hbl	Mg-Hbl	Mg-Hbl	Mg-Hbl	Mg-Hbl	Mg-Hbl	Act	Mg-Hbl	Mg-Hbl
T (ideally 8 apfu)									
Si	7.277	7.081	7.248	7.268	7.052	7.17	7.452	7.173	7.131
Al	0.723	0.919	0.752	0.732	0.948	0.83	0.548	0.827	0.869
T subtotal	8	8	8	8	8	8	8	8	8
C (ideally 5 apfu)									
Ti	0.042	0.037	0.034	0.034	0.056	0.038	0.024	0.04	0.051
Al	0.425	0.5	0.463	0.427	0.477	0.474	0.375	0.483	0.431
Cr	0.005	0.046	0.032	0.021	0.028	0.026	0.026	0.003	0.007
Fe3+	0.038	0.054	0.019	0.042	0.059	0.032			0.066
Ni	0.003	0.005	0.003		0.002	0.005	0.002		0.003
Mn2+	0.007	0.006	0.014	0.009	0.003	0.012	0.017	0.018	
Fe2+	0.945	0.916	0.909	0.871	0.924	0.943	0.833	0.961	0.916
Mg	3.535	3.436	3.525	3.596	3.451	3.471	3.718	3.495	3.525
C subtotal	5	5	4.999	5	5	5.001	4.995	5	4.999
B (ideally 2 apfu)									
Mn2+	0.011	0.015	0.005	0.012	0.017	0.009			0.018
Ca	1.931	1.943	1.94	1.936	1.935	1.951	1.956	1.98	1.946
Na	0.058	0.042	0.055	0.052	0.049	0.04	0.044	0.02	0.035
B subtotal	2	2	2	2	2.001	2	2	2	1.999
A (from 0 to 1 apfu)									
Na	0.227	0.283	0.222	0.224	0.317	0.26	0.149	0.278	0.297
K	0.002	0.004	0.002	0.002	0.004	0.002	0.002	0.004	0.002
A subtotal	0.229	0.287	0.224	0.226	0.321	0.262	0.151	0.282	0.299
O (non-W)	22	22	22	22	22	22	22	22	22
W (ideally 2 apfu)									
OH	2	2	2	2	2	2	2	2	2
W subtotal	2	2	2	2	2	2	2	2	2
Sum T,C,B,A	15.229	15.287	15.223	15.226	15.322	15.263	15.146	15.282	15.297
Altot	1.148	1.419	1.215	1.159	1.425	1.304	0.923	1.31	1.3
P	2.19	2.97	2.37	2.22	2.99	2.62	1.65	2.64	2.61

Table 3. Composition of the pyroxene from the metamorphic sole rocks of Kömürhan ophiolite (continued).

Temperature based on Ti (Otten, 1984) - warning: semi empirical; best used to determine magmatic versus secondary compositions									
T (C) Ti-hbld	779.269 9748	758.510 7585	759.258 3878	770.487 1664	781.608 1973	757.842 6965	759.364 0939	744.855 5743	780.186 0399

Number of ions on the basis of 23 oxygens. Total Fe is expressed as FeO*.

Table 3. Composition of the plagioclase from the metamorphic sole rocks of Kömürhan ophiolite.

Sample	KMF-1	KMF-2	KMF-3	KMF-4	KMF-5	KMF-6	KMF-7	KMF-8	KMF-9	KMF-10	KMF-11	KMF-12
SiO_2	31.42	48.96	49.22	41.66	45.64	48.95	46.66	47.92	48.99	46.09	67.01	49.2
Al_2O_3	1.27	32.96	32.86	33.78	34.4	33.45	34.92	33.96	33.18	35.14	20.56	32.53
TiO_2	37.44	0	0	0	0	0	0	0	0	0	0	0
FeO	0.46	0.03	0.02	0.34	0.06	0.04	0.08	0.03	0.03	0.06	0.07	0.02
MnO	0.03	0	0	0	0	0	0	0	0	0.02	0	0
MgO	0.41	0	0	0.02	0	0	0	0	0	0	0	0.02
CaO	27.76	15.12	14.97	22.74	18.31	15.31	17.19	16.16	15.18	18.13	0.79	14.55
Na_2O	0	2.85	2.94	0.56	1.36	2.74	1.69	2.41	2.83	1.49	11.07	3.16
K_2O	0.01	0	0.01	0.02	0	0.01	0	0	0	0	0.01	0
TOTAL	98.96	99.95	100.07	99.13	99.79	100.55	100.58	100.53	100.22	100.95	99.51	99.48
Cations												
Si	1.71	2.23	2.24	1.94	2.10	2.22	2.13	2.18	2.23	2.10	2.95	2.25
Al^{IV}	1.29	0.77	0.76	1.06	0.90	0.78	0.87	0.82	0.77	0.90	0.05	0.75
Al^{VI}	-1.21	1.01	1.01	0.80	0.97	1.01	1.01	1.00	1.01	0.98	1.02	1.00
Ti	1.53	0.00	0.00	0.00	0.00	0.00	0.00	0.00	0.00	0.00	0.00	0.00
Fe^{2+}	0.02	0.00	0.00	0.01	0.00	0.00	0.00	0.00	0.00	0.00	0.00	0.00
Mn	0.00	0.00	0.00	0.00	0.00	0.00	0.00	0.00	0.00	0.00	0.00	0.00
Mg	0.03	0.00	0.00	0.00	0.00	0.00	0.00	0.00	0.00	0.00	0.00	0.00
Ca	1.62	0.74	0.73	1.14	0.90	0.74	0.84	0.79	0.74	0.88	0.04	0.71
Na	0.00	0.25	0.26	0.05	0.12	0.24	0.15	0.21	0.25	0.13	0.94	0.28
K	0.00	0.00	0.00	0.00	0.00	0.00	0.00	0.00	0.00	0.00	0.00	0.00
Total	5.00	5.00	5.00	5.00	5.00	5.00	5.00	5.00	5.00	5.00	5.00	5.00
Or	0.04	0.00	0.06	0.10	0.00	0.06	0.00	0.00	0.00	0.00	0.06	0.00
Ab	0.00	25.43	26.21	4.26	11.85	24.45	15.10	21.25	25.23	12.95	96.15	28.21
An	99.96	74.57	73.74	95.64	88.15	75.49	84.90	78.75	74.77	87.05	3.79	71.79

Number of ions the basis of 8 oxygens. Total Fe is expressed as FeO*.

rams were proposed to discriminate orogenic from nonorogenic suites (Ca versus Ti+Cr), subalkali from alkaline basalts (Ti versus Ca + Na), and tholeiitic orogenic from calc-alkaline orogenic suites (Ti versus Al) (Figs. 5b–d). Based on these useful discrimination diagrams, it can be seen that the analysed pyroxene samples are all plotted in the field of orogenic suite (Fig. 5b). These clinopyroxenes are also expressly alkaline basalts (Fig. 5c). The examined pyroxenes with tholeiitic compositions lie certainly in the orogenic subfield (Fig. 5d). Based on [32] discrimination diagrams, metamorphic sole seen to be orogenic attitude together with an intense tholeiitic characteristic. Electron microprobe analysis compositions show that almost all feldspars are bytownite (An_{71-88}) in amphibolite, while rare feldspar samples are anorthite (An_{96-99}) and also an example is albite (An_4) (Fig. 6a) (Table 3). Hornblend is the dominant component in the metamorphic sole rocks of Kömürhan ophiolite, in particular, those from the south–eastern district of Kömürhan ophiolite. Mineralogically heterogeneous crystals presenting varying colours from field to field inside individual crystal have been avoided for EPMA. The characteristical magnesio–hornblendes are described by SiO_2=49.32–52.65%, Al_2O_3=5.53–8.46%, TiO_2=0.23–0.52%, MgO=16.08–17.62%, FeO=7.04–8.23%, K_2O=0.01–0.02% and overall the examined amphiboles are presenting a magnesian character together with a limited range of Mg number ($Mg^{\#}$=Mg/(Mg + Fe2+) are ranging from 78 to 82 and of a

Table 4. Composition of the titanite from the metamorphic sole rocks of Kömürhan ophiolite

Sample	KMT-1	KMT-2	KMT-3
SiO_2	30.88	30.84	30.86
TiO_2	37.14	37.61	38.25
Al_2O_3	1.65	1.31	1.03
Cr_2O_3	0.12	0.11	0.16
FeO	0.42	0.42	0.38
MnO	0.05	0.05	0.03
MgO	0.06	0.00	0.02
CaO	27.83	27.91	27.86
Na_2O	0.00	0.00	0.00
K_2O	0.00	0.00	0.00
TOTAL	98.16	98.28	98.61
Notes	titanite	titanite	titanite
Si	2.03	2.03	2.03
Ti	1.84	1.86	1.89
Zn	0.00	0.00	0.00
Al	0.13	0.10	0.08
Cr	0.01	0.01	0.01
Fe	0.02	0.02	0.02
Ni	0.00	0.00	0.00
Mn	0.00	0.00	0.00
Mg	0.01	0.00	0.00
Ca	1.96	1.97	1.96
Na	0.00	0.00	0.00
K	0.00	0.00	0.00
O	9.94	9.95	9.97
Cations	6.00	6.00	6.00

calcic affinity ([Na + Ca]B > 1 and [Na]B < 0.5). According to discrimination diagrams of [33], examined amphiboles from sole rocks of Kömürhan ophiolite can be chemically defined as magnesio–hornblende (Fig. 6b).

Seeing that whole metamorphic sole rocks examined are extensively mafic in character, their mineral assemblages have been ideally indicated by the ACF discrimination diagram (Fig. 7a) which is suggested by [34]. The studied amphibolite facies of metamorphic sole rocks mostly plotted in the diopside and hornblende zone of mafic rocks. [35] reported the semi-quantitative geobarometer to state the pressure evolution of hornblendes from the metamorphic rocks. The calculated pressures were less than 0.5 GPa. The estimated pressure for the examined rocks, calculated from the contents of the Al^{IV} versus Na^{M4} a.p.f.u. numbers from hornblendes, was 2-5 kbar (Fig. 7b). The pattern of Al^{IV}/Ti ratios from the examined amphiboles Al^{IV} versus Ti diagram presents that the participation of the contamination and magma mixing role in the geodynamic evolution of the analyzed rocks (Fig. 7c). Hornblendes from metamorphic and igneous processes have been categorized by Al^{VI} vs. Al^{IV} diagram [36]. The examined hornblendes from the studied rocks are metamorphic origin, derived by the metamorphic process (Fig. 7d).

DISCUSSION

The best observed stratigraphic–tectonomagmatic units of Southeast Turkey in the Cretaceous have been (i) op-

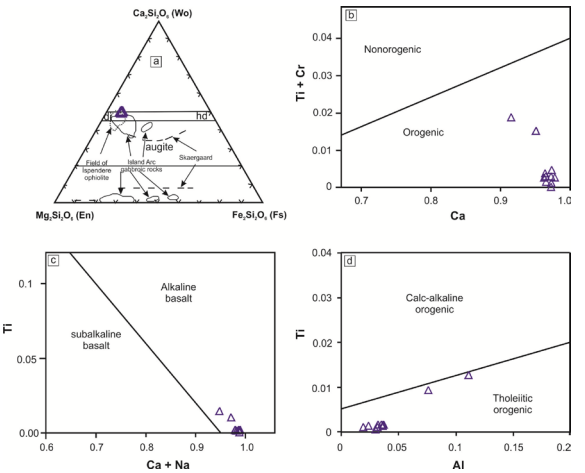

Figure 5. (a) Clinopyroxene major element compositions. (b) Plot of Ti + Cr versus Ca proposes that the metamorphic sole rocks from orogenic composition. Nonorogenic, orogenic, subalkaline, alkaline, calcalkaline and tholeiitic subfields are after [32].

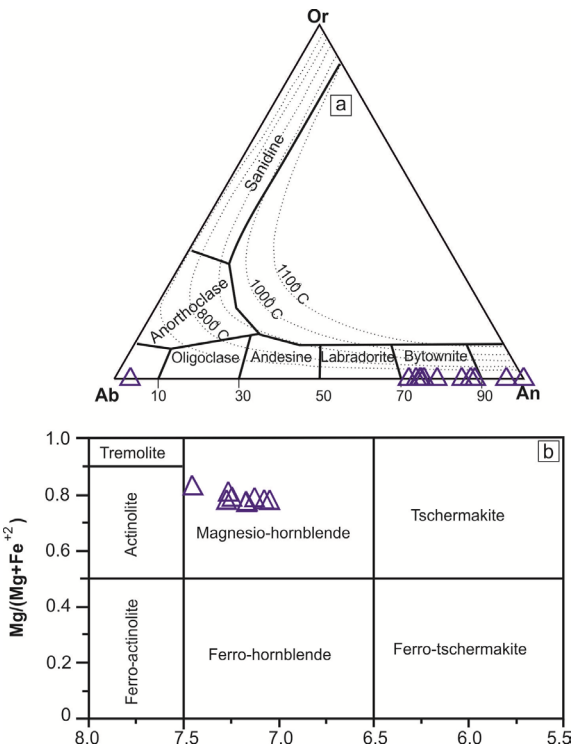

Figure 6. (a) Or-Ab-An discrimination diagram for feldspar (after Leake and Woolley Arps 1997) b) Amphibole discrimination diagram for (Na+K)A < 0.5 (a) and (Na + K)A > 0.5 (b) (after [33]).

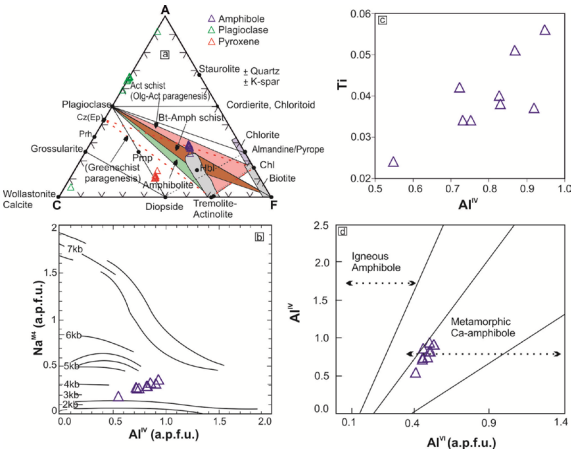

Figure 7. (a) Mineral assemblages of the amphibolites from Kömürhan ophiolite are shown in the ACF diagram (Best 1982). A = Al_2O_3 + Fe_2O_3 ± (Na_2O + K_2O); C = CaO−3,3 P_2O_5; F = FeO+MgO+MnO. (b) Comparison of Na^{M4} and Al^{IV} positions for amphibole from Metamorphic sole rocks of the Kömürhan ophiolite (after [29]). The mineral chemistry data of the amphiboles from the Kömürhan ophiolite: (c) Al^{IV} versus Al^{VI} diagrams (after Fleet and Barnett, 1978); (d) Plot of amphibole data on Ti versus Al^{IV} diagram (after [33]).

hiolites (e.g. İspendere, Guleman, Kömürhan Göksun), (ii) metamorphic massifs (e.g. Keban, Malatya metamorphics), (iii) granitic bodies (e.g. Baskil granitoid) and volcanic arcs (e.g. Elazığ–Yüksekova magmatics). The SAOB geodynamic evolution included onward relative movement of the nappes which contain both ophiolitic and metamorphic massifs, towards the Arabian platform throughout from Late Cretaceous to Miocene time interval [37, 16, 17, 38, 47]. Malatya–Keban metamorphics is a unit with low-grade metamorphism that rarely contains metaconglomerate, together with marble, schist, slate, and black phyllites [39,17]. Sheeted dykes and isotropic gabbros of Kömürhan ophiolite are tholeiitic in character (Nb/Y=0.2–0.06), and rare earth element (REE) spider and tectonomagmatic discrimination diagrams suggest that these rocks are formed in a supra-subduction zone geodynamic setting [23, 29]. Rızaoğlu et al. (2006) also reported that the metamorphic sole rocks of the Kömürhan ophiolite present tholeiitic in character (Nb/Y=0.07–0.33) and Rare earth element (REE)–spider diagram and tectonomagmatic discrimination diagrams indicate that these rocks have an island arc character. The Kömürhan ophiolite was formed in the Late Cretaceous (~ 90 My) between the Arabian platform in the south and the Taurus platform in the north, on a supra-subduction zone tectonic setting in the southern branch of Neotethys [23, 29]. Clinopyroxenes in the metamorphic sole rocks are of affinity because these mafic minerals are constantly resisting in retrogressive metamorphism and such other mafic minerals are converted to epidote and/or chlorite-type secondary minerals. Many researchers developed several discrimination/variation diagrams for clinopyroxenes based on their major and minor element compositions [40, 32, 41]. These diagrams allow researchers to evaluate the origin of metamorphic sole rocks, together with the aim of defining the geodynamic setting of Kömürhan ophiolite. Rızaoğlu et al. (2006) reported that volcanics mainly basaltic of the Kömürhan ophiolite present tholeiitic in nature depend on their Nb/Y ratios (0.5–0.02). These basaltic volcanics are thought to be protolith of metamorphic sole rocks, which are the main subject of research. The hornblende structural formulae have been conducted on the basis of the ACES2013 Excel spreadsheet [36], whereas Inverse thermobarometry has been calculated by using the basis of the Ti in–hornblende and amphibole–plagioclase compositions [43, 44] Whole hornblende compositions, presented in Table 1. have been calculated by operating the Excel spreadsheet for the Al–in–hornblende geobarometry [45] and also Hbl-Pl thermobarometry; the calculation equation is 0.5 + (0.331 × Altot) + [0.995 × (Altot × Altot)] [45, 46]. ISOPLOT 4.15 Excel add–in has been used for the inverse geothermobarometry [46] and the data provided by this method have been used for weighted average calculations of the P-T status. For examined hornblendes from the metamorphic sole rocks the inverse geothermobarometry models given a weighted average value of 2.48 ± 0.33 kbar (95 % conf., MSWD = 0.71, probability= 0.68). For magnesio–hornblendes from the metamorphic rocks, the temperatures are ranging from 744.9 ± 40 °C to 781.0 ± 40 °C with a weighted mean value of 766.0 ± 26 °C (95 % conf., MSWD =0.102, probability= 0.999).

CONCLUSION

From the outcomes of this analysis and the subsequent discussion, the following conclusions were drawn.

- The metamorphic sole rocks of Kömürhan ophiolite are composed of four main lithologies; amphibolite (Pl+Mg–Hbl+Ttn±Ap) plagioclase–amphibole schist (Pl+Mg–Hbl+Cpx+Ttn±Zrn±Ap), plagioclase–clinopyroxene-amphibole schist (Pl+Di+Mg–Hbl+Ttn±Ap), and epidote–plagioclase amphibole schist (Ep+Pl+Mg–Hbl+Ttn±Ap±Qtz±Zrn).

- The metamorphic sole rocks occurred as a result of the metamorphism of the island–arc tholeiite (IAT) type mafic rocks which separated from the upper section of the subducted ophiolitic crust and then dipped under the plate.

- The examined amphiboles in the metamorphic sole rocks of Kömürhan ophiolite experienced calculated temperatures of 744–781 °C throughout the metamorphism with a weighted average value of 766.0±26 °C as well as pressures of 1.65–2.99

kbar with a weighted mean value of 2.48±0.33 kb at an approximate depth of 8 km.

- The new petrographic, detailed mineral chemistry analyses, together with geochemical interpretations, and geothermobarometry estimates from the amphibole schist–amphibolites of Kömürhan ophiolite, suggest that these rocks occurred on a subducted slab during the ophiolite formations in a Supra-subduction zone geodynamic setting.

ACKNOWLEDGEMENT

The author would like to thank Dr. Andrew Locock for performing mineral chemistry analyses and The author is also indebted to the anonymous reviewers and the Editor for their constructive comments and suggestions, which greatly helped to improve the manuscript. Funding information: Financial supports from the Çukurova University Research Foundation (Project No: FBA- 2021-13093).

References

1. Williams H. and Smyth W.R. Metamorphic aureoles beneath ophiolite suites and Alpine peridotites: Tectonic implications with west Newfoundland examples. Am. J. Sci. 273, (1973) 594–621.
2. Coleman R.G. Tectonic setting for ophiolite obduction in Oman. J. Geophys. Res. 86, (1981) 2497–2508.
3. Searle M.P. and Cox J. Subduction zone metamorphism during formation and emplacement of the Semail ophiolite in the Oman Mountains. Geol. Mag. 139, 3, (2002) 241–255.
4. Nurlu, N. U–Pb zircon geochronology and geochemistry of the metamorphic sole rocks of the Meydan mélange, South-East Turkey: Implications for ophiolite emplacement and protolith, GEOLOGICA CARPATHICA, 71, 2, (2020) 183–205.
5. Al-Riyami K., Robertson A., Dixon J. and Xenophontos C. Origin and emplacement of the Late Cretaceous Baer–Bassit ophiolite and its metamorphic sole in NW Syria. Lithos 65, 1, (2002) 225–260.
6. Çelik Ö.F. Detailed geochemistry and K-Ar geochronology of the metamorphic sole rocks and their mafic dykes from the Mersin Ophiolite, Southern Turkey: Turk. J. Earth Sci. 17, (2008) 685–708.
7. Sayit, K., Bedi, Y., Tekin, U.K., Göncüoğlu, M.C., Okuyucu, C. Middle Triassic backarcbasalts from the blocks in the Mersin Mélange, southern Turkey: implications for thegeodynamic evolution of the Northern Neotethys. Lithos 268, (2017) 102–113.
8. Nurlu, N. Petrology and LA-ICP-MS zircon geochronology for Late Cretaceous felsic dikes and intermediate volcanic rocks hosted in Mersin ophiolite, South Turkey and its implications. Geosci J (2020). https://doi.org/10.1007/s12303-020-0020-0.
9. Guilmette, C., Smit, M.A., van Hinsbergen, D.J.J., Gürer, D., Corfu, F., Charette, B., Maffione, M., Rabeau, O., and Savard, D. Forced subduction initiation recorded in the sole and crust of the Semail Ophiolite of Oman: Nature Geoscience, v. 11, p. (2018) 688–695, https:// doi.org/10.1038/s41561-018-0209–2.
10. Kim, S., Jang, Y., Kwon, S, Samuel, O. V., Kim, S.W., Park, S., Santosh, M., Kokkalas, S. Petro-tectonic evolution of metamorphic sole of the Semail ophiolite, UAE, Godwana Research, 86 v, (2020) p. 203–221.
11. Howard, D. P. Unravelling ophiolite emplacement history with microfossils - the Baer-Bassit ophiolite of NW Syria. Doctoral thesis, UCL (University College London). (2006) p. 1–232.
12. Chan, G. H., Malpas, J., Xenophontos, C., Lo, C. H. Timing of subduction zone metamorphism during the formation and emplacement of Troodos and Baer–Bassit ophiolites: insights from 40Ar–39Ar geochronology. Geol. Mag. 144 (5), 2007, pp. 797–810.
13. Lytwyn J.N and Casey J.F. The geochemistry of post kinematic mafic dyke swarms and subophiolitic metabasites, Pozanti–Karsanti ophiolite, Turkey: Evidence for ridge subduction. Geol. Soc. Am. Bull. 107, (1995) 830–850.
14. Gnos E., and Peters T. K–Ar ages of the metamorphic sole of the Semail ophiolite: implications for cooling history. Contrib. Mineral. Petrol. 113, (1993) 325–332.
15. Şengör A.M.C. and Yılmaz Y. Tethyan evolution of Turkey: A plate tectonic approach. Tectonophysics 75, (1981) 181–241.
16. Yilmaz, Y. New evidence and model on the evolution of the southeast Anatolian orogen. Geological Society of America Bulletin, 105, (1993) 251–271.
17. Yilmaz Y., Yiğitbaş E. and Genç Ş.C. Ophiolitic and Metamorphic Assemblages of Southeast Anatolia and their Significance in the Geological Evolution of the Orogenic Belt. Tectonics 12, (1993) 1280–1297.
18. Robertson, A. H. F., Ustaömer, T., Parlak, O., Ünlügenç, U. C., Tasli, K. and İnan, N. The Berit transect of the Tauride thrust belt, S. Turkey: Late Cretaceous–Early Cenozoic accretionary/ collisional processes related to closure of the Southern Neotethys. Journal of Asian Earth Sciences. (2006)
19. Robertson A.H. F., Parlak O., Rizaoğlu T., Ünlügenç Ü., İnan N., Tasli K. and Ustaömer T. Tectonic evolution of the South Tethyan ocean: evidence from the Eastern Taurus Mountains (Elazığ region, SE Turkey). Geol. Soc. London, Spec. Publ. 272, (2007) 231–270.
20. Yazgan E. and Chessex R. Geology and Tectonic Evolution of the South–eastern Taurides in the Region of Malatya. Turk. Assoc. Petrol. Geol. 3, (1991) 1–42.
21. Bağcı U., Parlak O. and Höck V. Whole-Rock Mineral Chemistry of Cumulates from the Kızıldağ (Hatay) Ophiolite (Turkey): Clues for Multiple Magma Generation During Crustal Accretion in the Southern Neotethyan Ocean. Mineral. Mag. 69, 1, (2005) 53–76.
22. Beyarslan M. and Bingöl A.F. Petrology of a suprasubduction zone ophiolite (Elazığ, Turkey). Canad. J. Earth Sci. 37, (2000) 1411–24.
23. Rızaoğlu, T., Parlak, O., Höck, V., İşler, F. Nature and significance of Late Cretaceous ophiolitic rocks and its relation to the Baskil granitoid in Elazığ region, SE Turkey. In Tectonic Development of the Eastern Mediterranean, Robertson, A.H.F., Mountrakis, D. (eds). Geological Society, London, Special Publication, 260: (2006) 327–350.
24. Parlak O., Rizaoğlu T., Bağci U., Karaoğlan F. and Höck V. Tectonic significance of the geochemistry and petrology of ophiolites in southeast Anatolia, Turkey. Tectonophysics 473, (2009) 173–187.
25. Nurlu N. Geochemistry and Tectonic Signifiance of the Tectonomagmatic Units in the Helete (Kahramanmaraş) Region. PhD Thesis, Çukurova University Intitute of Natural and Applied Sciences, (2016) 1–281. (in Turkish with English abstract).
26. Nurlu N., Parlak O., Robertson A.H.F. and Quadt A. Implications of Late Cretaceous U–Pb zircon ages of granitic intrusions cutting ophiolitic and volcanogenic rocks for the assembly of the Tauride allochton in SE Anatolia (Helete area, Kahramanmaraş Region, SE Turkey). Int. J. Earth Sci. 105, (2016) 283–314.
27. Robertson A.H.F. Overview of the genesis and emplacement of Mesozoic ophiolites in the eastern Mediterranean Tethyan region.

Lithos 65, (2002) 1–67.
28. MTA (General Directorate of Mineral Research and Exploration). 1:500.000 scaled 513 Geological Maps of Turkey (Adana map section), Ankara-Turkey. (2002) (in Turkish with 514 English abstract) http://www.mta.gov.tr/eng/maps/geological–500000 .
29. Rızaoğlu, T. Petrography and Geochemistry of the Tectonomagmatic Units Cropping Out Between Baskil and Sivrice (Elaziğ), PhD Thesis, Çukurova University Intitute of Natural and Applied Sciences,(2006) 1–259. (in Turkish with English abstract).
30. Donovan J.J., Snyder D.A and Rivers M.L. An Improved Interference Correction for Trace Element Analysis. Microbeam Analysis 2, (1993) 23–28.
31. Armstrong J.T. Quantitative analysis of silicates and oxide minerals: Comparison of Monte-Carlo, ZAF and Phi-Rho-Z procedures. In: Newbury D.E. (Ed.): Microbeam Analysis. San Francisco Press, (1988) 239–246.
32. Leterrier, J., Maury, R., Thono, P., Girard, D., and Marchal, M. Clinopyroxene composition as a method of identification of the magmatic affinities of paleovolcanic series: Earth and Planetary Science Letters, v. 59, p. (1982) 139–154.
33. Leake B.E., Woolley A.R., Arps C.E.S., Birch W.D., Gilbert M.C., Grice J.D., Hawthorne F.C., Kato A., Kisch H.J., Krivovichev V.G., Linthout K., Laird J., Mandarino J.A., Maresch W.V., Nickel E.H., Rock N.M.S., Schumacher J.C., Smith D.C., Stephenson N.C.N., Ungaretti L., Whittaker E.J.W. and Youzhi G., Nomenclature of amphiboles; Report of the Subcomm. on Amphiboles Intern. Miner. Ass., Commiss. New Minerals and Mineral Names. Am. Mineral., 82: (1997) 1019-1037.
34. Best M. G. Igneous and metamorphic petrology. Freeman, San Francisco, USA, (1982) 1–458.
35. Brown E.H. The crossite content of ca-amphibole as a guide to pressure of metamorphism. J. Petrol. 18, (1977) 53–72. https://doi.org/10.1093/petrology/18.1.53
36. Fleet, M.E., Barnett, R.L. Partitioning in calciferous amphiboles from the Frood Mine, Sudbury, Ontario. Can. Mineral. 16, (1978) 527–532.
37. Yildirim, M. and Yilmaz, Y. Güneydogu Anadolu orojenik kuşağının ekaylı zonu. Bulletin of Turkish Association of Petroleum Geologists, 3, (1991) 57–73. (in Turkish with English abstract).
38. Robertson, A. H. F., Ustaömer, T., Parlak, O., Ünlügenç, U. C., Tasli, K. and İnan, N. The Berit transect of the Tauride thrust belt, S. Turkey: Late Cretaceous–Early Cenozoic accretionary/ collisional processes related to closure of the Southern Neotethys. Journal of Asian Earth Sciences. (2006)
39. Turan, M., Ve Bingöl, A. F. Kovancılar-Baskil (Elazığ) Arası Bölgenin Tektono-stratigrafik Özellikleri. Ahmet Acar Jeoloji Sempozyumu, Bildiriler, Çukurova Üniversitesi, Adana, (1991) 213–227. (in Turkish with English abstract).
40. Nisbet, E., and Pearce, J. Clinopyroxene composition in mafic lavas from different tectonic settings: Contributions to Mineralogy and Petrology, v. 63, p. (1977) 149–160.
41. Beccaluva, L., Macciotta, G., Piccardo, G.B., and Zeda, O. Clinopyroxene composition of ophiolite basalts as petrogenic indicator: Chemical Geology, v. 77, p. (1989) 165–182
42. Locock A.J. 2014: An Excel spreadsheet to classify chemical analyses of amphiboles following the IMA 2012 recommendations. Comput. Geosci. 62, 1–11.
43. Johnson M.C. and Rutherford M.J. Experimental calibration of the aluminum in hornblende geobarometer with application to long valley caldera (California) Volcanic Rocks. Geology 17, (1989) 837–841.
44. Holland T. and Blundy J. Non-ideal interactions in calcic amphiboles and their bearing on amphibole-plagioclase thermometry. Contrib. Miner. Petrol. 116, (1994) 433–447.
45. Anderson J.L., Barth A.P., Wooden J.L. and Mazdab F. Thermometers and thermobarometers in granitic systems. Rev. Mineral. Geochem. 69, 1, (2008) 121–142.
46. Ludwig K.R. User's Manual for Isoplot 3.00: A Geochronological Toolkit for Microsoft Excel. Special Publication/Berkeley Geochronology Center (2003) 74.
47. Nurlu N. U–Pb zircon geochronology and geochemistry of the metamorphic sole rocks of the Meydan mélange, South-East Turkey: Implications for ophiolite emplacement and protolith. Geologica Carpathica, 71, 2, (2020) 183–205.
48. Akıncı A. C., Robertson A. H. F., Ünlügenç U. C. Late Cretaceous–Cenozoic subduction–collision history of the Southern Neotethys: new evidence from the Çağlayancerit area, SE Turkey. International Journal of Earth Sciences 105, (2016) 315-337